

Polarization of Recoil Protons from Neutral Pion Photoproduction*

D. E. LUNDQUIST,† R. L. ANDERSON, J. V. ALLABY,‡ AND D. M. RITSON

High Energy Physics Laboratory, Stanford University, Stanford, California

(Received 23 October 1967)

The polarization of recoiling protons from the photoproduction of π^0 mesons on liquid hydrogen has been measured for primary photon energies between 500 and 1000 MeV over a range of π^0 c.m. angles from 55° to 130° . The results show structure not observed previously in experiments of less precision. In particular, the polarization at 90° c.m. is close to zero at a primary photon energy of 900 MeV. Also, a strong dependence of polarization on π^0 c.m. angle between 600 and 900 MeV was observed. A subsidiary measurement of the polarization of the recoil protons from elastic e - p scattering at 900 MeV and $q^2=10$ F $^{-2}$ gave a value $(1.3\pm 2.0)\%$.

1. INTRODUCTION

OVER the last several years, detailed measurements of pion-nucleon total, elastic, and charge-exchange cross sections, recoil nucleon polarizations, and measurements with polarized targets have revealed a wealth of detail in the pion-nucleon phase shifts below 1-GeV pion lab energy.¹ Photoproduction of pions from single nucleons is dominated by the interaction of the pion with the nucleon in the final state, and is closely related to pion-nucleon scattering.

In order to separate the real and imaginary parts of the various partial-wave amplitudes present in the photoproduction of mesons, it is necessary to study not only the cross sections, but also the polarizations of recoiling nucleons. We have studied the polarization of recoiling protons from hydrogen, produced in association with single neutral pions, as a function of energy and angle. For a given primary photon energy, k , the measured polarization, $P(k, \theta_\pi)$, of the proton times the differential production cross section $d\sigma(k, \theta_\pi)/d\Omega$, can be expanded in polynomial coefficients in $\cos\theta_\pi$ in the form

$$\frac{P(k, \theta_\pi) d\sigma(k, \theta_\pi)/d\Omega}{\sin\theta_\pi} = A(k) + B(k) \cos\theta_\pi + C(k) \cos^2\theta_\pi + \dots, \quad (1)$$

where θ_π is the c. m. angle of the pion. The $A(k)$ and $C(k)$ coefficients are sensitive only to interferences between states of opposite parity, and the $B(k)$ coefficient only to interferences between states of the same parity.² If only two final states are present, then the interference is also proportional to the sine of the relative phase difference between the two amplitudes.

* Work supported in part by the U. S. Office of Naval Research Contract No. Nonr 225(67).

† Present address: Argonne National Laboratory, Argonne, Ill.

‡ Present address: CERN, Geneva, Switzerland.

¹ This is not a complete compilation of pion-nucleon phase-shift analyses, but it is representative of the major groups engaged in phase-shift analyses: L. David Roper, Robert M. Wright, and Bernard T. Feld, *Phys. Rev.* **138**, B190 (1965); B. H. Bransden, P. J. O'Donnell, and R. G. Moorhouse, *ibid.* **139**, B1566 (1965); P. Auvil, C. Lovelace, A. Donnachie, and A. T. Lea, *Phys. Letters* **12**, 76 (1964); P. Bareyre, C. Brickman, A. V. Stirling, and G. Villet, *ibid.* **18**, 342 (1965).

² R. F. Peierls, *Phys. Rev.* **118**, 325 (1960).

Stein³ at Cornell performed the first proton-polarization experiments at primary photon energies of 550 and 700 MeV at 90° c. m. and showed that the "second" resonance (1512 MeV) has opposite parity to that of the first at 1236 MeV. Later, measurements at Frascati⁴ and at the Stanford Mark III accelerator by a Caltech-Stanford-Pisa collaboration⁵ were extended to show the variation with energy of the polarization at 90° c.m. These measurements suffered from a lack of energy resolution, so that they missed some of the structure subsequently observed in this experiment. This experiment used primary photons in the energy range 500–1000 MeV. In the energy range 600–900 MeV it covered a wide range of c.m. angles with the objective of determining both the coefficients A and B , and their variation with energy.

Recoiling protons produced by a photon beam incident on a liquid-hydrogen target were analyzed in momentum and angle with either one of two magnetic spectrometers. Protons emerging from the spectrometers scattered to the left or right from a carbon analyzer. The proton polarization was measured from the left-right asymmetry in the scattering from the carbon analyzer. Instrumental asymmetries which could have produced an artificial asymmetry were almost totally eliminated by making measurements with the spectrometer alternated symmetrically on either side of the photon-beam axis.

2. EXPERIMENTAL

The high-intensity beam of momentum-analyzed electrons from the Stanford Mark III linear accelerator was used to produce a beam of bremsstrahlung photons for the photoproduction experiment. Figure 1 shows the layout of the photoproduction experiment. In one arrangement (not shown in Fig. 1) the electron beam

³ P. C. Stein, *Phys. Rev. Letters* **2**, 473 (1959).

⁴ R. Querzoli, G. Salvini, and A. Silverman, *Nuovo Cimento* **19**, 53 (1961); C. Mencuccini, R. Querzoli, and G. Salvini, *Phys. Rev.* **126**, 1181 (1962); L. Bertanza, P. Franzini, I. Mennelli, and G. V. Silvestrini, *Nuovo Cimento* **19**, 953 (1961).

⁵ J. O. Maloy, Ph.D. thesis, California Institute of Technology, 1961 (unpublished); J. O. Maloy, G. A. Salandini, A. Manfredini, V. Z. Peterson, J. I. Friedman, and H. Kendall, *Phys. Rev.* **122**, 1338 (1961); J. O. Maloy, V. Z. Peterson, G. A. Salandini, F. Waldner, A. Manfredini, and H. Kendall, *ibid.* **139**, B733 (1965).

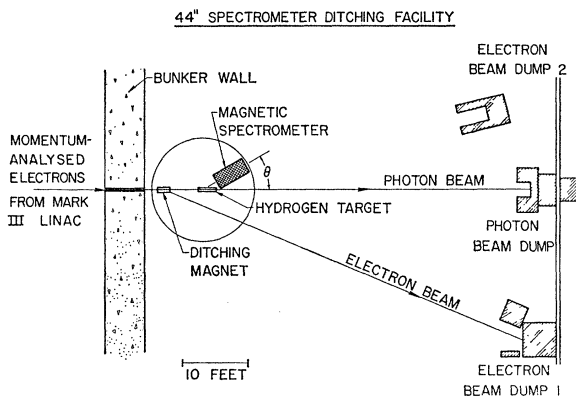


FIG. 1. Layout of the apparatus. The spectrometer and detectors were mounted on a rotatable gunmount and could be rotated on either side of the beam axis. The electron beam could be ditched either in "dumps" 1 or 2.

struck a copper radiator (about 0.1 of a radiation length thick) placed directly upstream from the hydrogen target. Both the electron beam and the resulting photon beam passed through the liquid hydrogen. However, during most of the runs the copper radiator was moved about 66-in. upstream from the hydrogen target and a "ditching" magnet was interposed between the radiator and the target so that only photons passed through the target, as shown in Fig. 1. When the spectrometer was at an angle θ on one side of the hydrogen target, the electron beam was swept by the magnet into beam dump area No. 1. Upon reversing the spectrometer to an angle $360^\circ - \theta$ on the other side, the current in the ditching magnet was also reversed to sweep the electron beam into beam dump area No. 2, on the opposite side of the photon beam.

The momentum and angle of the recoiling protons from the liquid-hydrogen target were selected by a 90° magnetic spectrometer.⁶ For measurements below 700 MeV/c, the HEPL 44-in. spectrometer was used. Measurements above 700 MeV/c were carried out

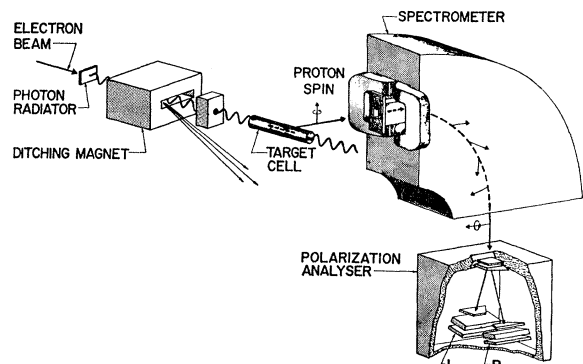


FIG. 2. Passage of the recoil protons through the spectrometer and the location of the detector system relative to the spectrometer.

⁶ J. V. Allaby and D. M. Ritson, Rev. Sci. Instr. 36, 607 (1965).

using the HEPL 100-in. spectrometer. For both magnets, the bend is in the vertical plane. Figure 2 shows a cutaway view of the 44-in. apparatus. At the target the spin of the photoproduced protons must be normal to the plane defined by the incident photon and recoil proton momenta (parity conservation). As the protons passed through the spectrometers, their spins precessed in the magnetic field by an angle α with respect to their direction of motion. The spin-precession angle α in our experiment varied between about 180° to 216° , depending on the path through the spectrometer and the momentum of the particle. If γ is the ratio of the total energy to the mass of the proton, $g/2$ for the proton has the standard value of 2.793, and b is the angular bend of the proton in the magnetic field of the spectrometer, the precession angle α is given by

$$\alpha = \gamma[(g/2) - 1]b. \quad (2)$$

After passage through the spectrometer, the protons registered in scintillation counter A placed in the spec-

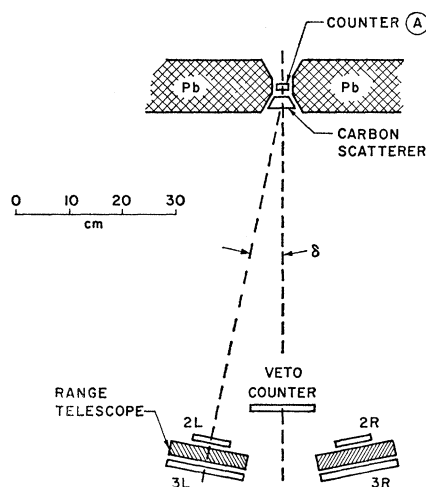


FIG. 3. Details of the polarization analyzer and the counter systems. The carbon scattering angle δ could be changed to give maximum analyzing power.

trometer focal plane, as shown in Fig. 3. The length of counter A defined the momentum acceptance of 3% in the 44-in. and 2% in the 100-in. spectrometer experiments. A carbon analyzer was placed just after counter A to produce the scattering necessary to analyze the proton polarization (see Fig. 3). Left and right scattering events from the carbon were identified in two identical two-counter range telescopes. Protons were identified by their characteristic pulse heights in each counter.

Artificial asymmetries between the left and right telescopes could be made to cancel by averaging the asymmetries measured on either side of the hydrogen target. This occurred because the proton spins at the production were normal to the production plane defined by $\mathbf{k}_\gamma \times \mathbf{q}_p$, where \mathbf{k}_γ is the incident photon momentum vector and \mathbf{q}_p is the recoil proton momentum vector.

When the spectrometer was changed from an angle θ on one side of the hydrogen target to an angle $-\theta$ on the other side, the proton polarization reversed; $P(-\theta) = -P(\theta)$. Instrumental asymmetries, however, did not reverse, and thus were cancelled by alternately running on either side of the hydrogen target and averaging the polarization measurements. If the measured scattering rates in the two telescopes are defined as shown schematically in Fig. 4, then the asymmetry ϵ which arises from the polarization of the protons is given by

$$\epsilon = \frac{[L(\theta) - R(\theta)] - [L(-\theta) - R(-\theta)]}{[L(\theta) + R(\theta)] + [L(-\theta) + R(-\theta)]}, \quad (3)$$

and is virtually independent of instrumental asymmetries.

3. BACKGROUNDS

The rates for scattering of protons into the two telescopes were given by the prompt coincidence rates minus the delayed rates between counter A and the telescopes. The subtraction for delayed coincidences varied between about 3–15% of the prompt rates.

The singles rates in the largest counters, 3L and 3R of Fig. 3, contributed several percent (estimated) dead-time loss in each telescope. However, the singles rates were symmetric for reversal of the spectrometer from the angles θ to $-\theta$ on the other side of the hydrogen target. Therefore, the correction to the asymmetry [Eq. (3)] was much smaller than the estimated several-percent correction to the rate in each telescope. Both the singles rates and the average linac beam pulse duration were monitored during the experiment to make sure that the dead-time corrections never became large or asymmetric.

π^+ mesons passed through the spectrometer and entered the polarization analyzer for many of the data points taken in this experiment. However, the pulse-height requirements in counter A and in both counters in each telescope were sufficient to clearly identify protons even in the presence of large π^+ backgrounds.

At the lower spectrometer momentum settings (543 MeV/c and below) and high machine energies (800 MeV and above) the signal of backward protons, from π^0 photoproduction at forward π^0 c.m. angles, was partially contaminated by particles whose flux depended directly on the presence of liquid hydrogen in the target. Such background fluxes, dubbed "ghost" protons by other workers,^{7–10} arise from secondary processes in the liquid hydrogen, and should not be appreciably polarized.

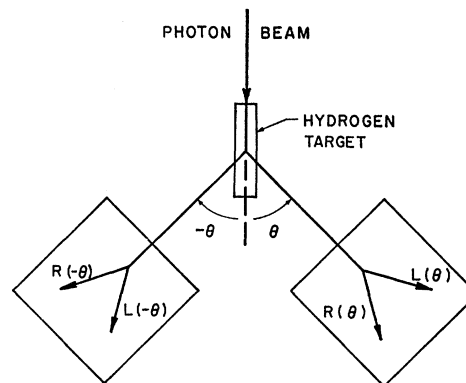


FIG. 4. "Conventions" used in Eq. (3) for the scattering yields on either side of the beam.

These liquid-hydrogen background protons could be separated from the π^0 protons by measuring their yield in kinematic regions where it was no longer possible for protons produced directly by π^0 photoproduction to appear. For instance, these hydrogen background protons could be detected by measuring the yield with the machine energy set below π^0 threshold; or, keeping the linac energy fixed, this background could be isolated by increasing the laboratory angle of the spectrometer until no more directly produced " π^0 " protons could appear in the spectrometer, as in Fig. 5. The measured polarization of these background particles was -0.08 ± 0.37 . We have subtracted the contribution due to

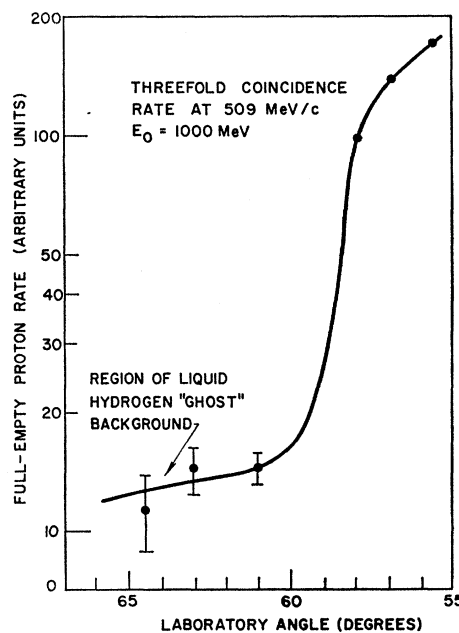


FIG. 5. Typical yield of counting rate versus laboratory angle. At laboratory angles above 60° , protons produced in association with π^0 mesons were kinematically forbidden for the momentum setting of the spectrometer. The protons appearing at angles greater than 60° resulted from double processes in the liquid hydrogen.

⁷ R. Diebold, Phys. Rev. **130**, 2089 (1963).

⁸ G. Bellettini, C. Bemporad, P. L. Braccini, L. Foà, and E. H. Bellamy, Nuovo Cimento **29**, 1195 (1963).

⁹ G. Bellettini, C. Bemporad, P. J. Biggs, P. L. Braccini, T. Del Prete, and L. Foà, Nuovo Cimento **44A**, 239 (1966).

¹⁰ Darrell J. Drickey and Robert F. Mozley, Phys. Rev. **136**, B543 (1964).

TABLE I. Typical settings for the carbon scatterer and the "left" and "right" telescopes used to detect the scattering asymmetry.

Spectrometer momentum (MeV/c)	Mean precession correction $\cos\alpha$	Thickness of the carbon scatterer (g/cm ²)	Angular acceptance for telescopes $\delta_{\min}-\delta_{\max}$	Mean analyzing power \bar{f}	Estimate of percentage uncertainty in \bar{f} $\frac{\Delta\bar{f}}{\bar{f}}$
433	-1.000	3.68	9°-15°	-0.180	10%
455	-0.990	3.61	13°-19°	-0.270	6%
459	-0.990	3.60	10°-18°	-0.260	6%
509	-0.982	3.61	11°-17°	-0.343	5%
543	-0.978	3.73	9°-15°	-0.472	3.6%
628	-0.950	5.24	8°-14°	-0.554	4%
684	-0.925	5.14	8°-14°	-0.658	3%
756	-0.883	10.00	9°-19°	-0.583	7%
831	-0.811	12.00	9°-19°	-0.417	4%

these background particles from the measured asymmetries of Eq. (3), assuming these background protons to have had zero polarization.

Empty-hydrogen-target background measurements were made by introducing an empty target cell into the photon beam in place of the full target cell. The target cell was a cylinder 12 in. long, 1.875 in. in diam with 0.002 in. stainless-steel walls whose axis was oriented along the beam direction. The lead collimator in Fig. 2 prevented the photon beam from striking the cylindrical side walls of the target, and neither the front- nor rear-end walls were viewed by the spectrometer. Empty target backgrounds varied from less than 1% at the highest momentum, to about 15% at the lowest momentum. The same hydrogen target was used for both the 44- and 100-in. spectrometer experiments.

For the data taken at 628-MeV/c spectrometer momentum setting, and for some of the data taken at 684 MeV/c, both the electron and photon beams passed through the hydrogen target cell. For these data it was necessary to correct for small backgrounds due to contamination by the "radiative tail" from elastic electron scattering.

4. EXPERIMENTAL PROCEDURE FOR DATA GATHERING

A thin, wobbling secondary emission monitor (SEM) was placed a few inches upstream from the radiator to monitor the intensity of the electron beam incident on the radiator. The photon-beam intensity was calculated from the known thickness of radiator in the beam. These intensity measurements were used to make crude checks of absolute rates and cross sections, and to ensure that the proton yields on either side of the photon beam were indeed equal.

To eliminate uncertainties in the knowledge of the carbon analyzing power that might have arisen from energy interpolations, momentum settings of the spectrometer (with two exceptions) were chosen to correspond to those energies at which polarized proton-carbon scattering experiments already existed. Polariza-

tion measurements were made on the bremsstrahlung plateau below the onset of two-pion production. At each momentum setting, the spectrometer angle was set to correspond to the desired primary photon energy. The linac energy was set 80-100 MeV higher than this energy, but never so high that the threshold was exceeded for the production of protons associated with the double pion photoproduction. For each datum point, the spectrometer was alternated several times between the angles θ and $-\theta$, so that artificial asymmetries could be averaged out as in Eq. (3).

5. CONVERSION OF MEASURED ASYMMETRIES TO POLARIZATION

Four scattering rates (indicated in Fig. 4) were measured for each datum point. From each of the individual prompt coincidence rates the random-coincidence rates were subtracted. Then the background protons from the empty-target, the liquid-hydrogen ghost-proton backgrounds, and possible elastic-scattering backgrounds were subtracted. The asymmetry ϵ_{π^0} was then computed from Eq. (3). The polarization P of these π^0 protons is given by

$$P = \epsilon_{\pi^0} / \bar{f}, \quad (4)$$

where \bar{f} is the mean analyzing power of the system, taking into account the precession of the spins described in Eq. (2). In computing the analyzing power it was necessary to utilize the extensive results on the scattering of polarized protons from carbon nuclei measured at many labs.¹¹⁻¹⁷ If the carbon analyzing power and unpolarized scattering cross section as a function of lab angle and proton energy are $a(\delta, E)$ and $\sigma(\delta, E)$, then the mean analyzing power \bar{f} is given by

$$\bar{f} = \frac{\sum \int \int \int \sigma(\delta, E) a(\delta, E) (\mathbf{s} \cdot \mathbf{n}) \sin \delta d\delta d\Phi dE}{\sum \int \int \int \sigma(\delta, E) \sin \delta d\delta d\Phi dE}, \quad (5)$$

where δ and Φ refer to the polar and azimuthal carbon scattering angle, and E refers to the energy at which

¹¹ J. M. Dickson and D. C. Salter, *Nuovo Cimento* **6**, 235 (1957). The first data of J. M. Dickson, B. Rose, and D. C. Salter [*Proc. Phys. Soc. (London)* **A68**, 361 (1955)] gave only asymmetry measurements with no report of polarizations.

¹² O. N. Jarvis, B. Rose, and J. P. Scanlon, *Nucl. Phys.* **77**, 161 (1966).

¹³ E. H. Thorndike, J. Lefrancois, and Richard Wilson, *Phys. Rev.* **120**, 1819 (1960); C. F. Hwang, T. R. Ophel, E. H. Thorndike, and Richard Wilson, *ibid.* **119**, 352 (1960); E. H. Thorndike and T. R. Ophel, *ibid.* **119**, 362 (1960). We have recomputed the beam polarizations in these experiments from the Dickson and Salter 135-MeV data as renormalized by Jarvis, Rose, and Scanlon. Then we have used this 6% lower beam polarization to compute polarization from the asymmetries reported in this reference. At 95 MeV, the renormalized Dickson-Salter data and the data of this reference then agree.

¹⁴ R. Althouse, A. Johansson, and G. Tibell, *Nucl. Phys.* **4**, 672 (1957).

¹⁵ H. Tyrén and Th. A. J. Maris, *Nucl. Phys.* **4**, 637 (1957).

¹⁶ W. G. Chesnut, E. M. Hafner, and A. Roberts, *Phys. Rev.* **104**, 449 (1956); E. M. Hafner, *ibid.* **111**, 297 (1958).

¹⁷ O. Chamberlain, E. Segre, R. D. Tripp, C. Wiegand, and T. Ypsilantis, *Phys. Rev.* **102**, 1659 (1956).

the scattering in the carbon block took place. Equation (2) was used to determine the direction of the unit spin vector \mathbf{s} before the scattering for the polarized protons impinging on the carbon scatterer; \mathbf{n} is the unit vector normal to the plane determined by the incident proton direction and the scattering. The range of integration over δ and Φ was determined by the position of the range telescope and the sizes of counter 2L or 2R. The integration interval in energy E was determined by the proton energy loss in the carbon. Inelastic scattering from the 4.4-MeV level of carbon was also included in the computation since the range telescopes were set to accept both elastic and inelastic events with up to 8–12 MeV energy loss.

Table I lists typical mean values of the precession correction used in the integrand of Eq. (5), and typical telescope angular-acceptance values. Exact values were generated by computer calculations during the course of evaluating the integrals of Eq. (5). Also listed in the thickness of the carbon scatterer, including the scintillator of counter A, and the estimated systematic uncertainty in the analyzing power. Finally, Table II lists the energy cutoffs set by the range telescope. The cutoff determines the inelastic excitation energy which the proton can give to the carbon nucleus. Energy losses for which the detection probabilities are 90 and 10%, respectively, are given.

6. RESULTS

As a check on the functioning of the apparatus, the polarization of the recoiling protons from elastic electron scattering were measured at a recoil proton momentum of 684 MeV/c. With the linac set at 900 MeV, the elastic proton peak was found by measuring the flux of protons as a function of laboratory angle on both sides of the photon beam. Running time was divided equally between measurements made at the top of the elastic peak on either side of the hydrogen target. The final asymmetry had to be corrected for an approximate 10% contamination by π^0 protons (in a range, however, where the π^0 polarization was measured and was close

TABLE II. Maximum energy losses for inelastic scattering from the carbon analyzer.

Spectrometer momentum (MeV/c)	Energy loss in MeV for 90% detection probability	Energy loss in MeV for 10% detection probability
433	3	7.5
455 (44-in. spectr)	10	14.5
455 (100-in. spectr)	4	6
509	6	12
543	3	8
628	7	19
684	7	14
758	2.5	6.5
831	3.5	12

TABLE III. Tabulation of polarization measurements taken with the 44-in. spectrometer.

Primary photon energy K_γ and resolution (HWHM) in MeV	$\cos\theta_{\pi^0\text{-m}}$	Experimental polarization values	Spectrometer momentum (MeV/c)
500±10	-0.105	0.107 ±0.093	509
500±9	-0.235	-0.248 ±0.075	543
549±10.5	+0.290	-0.014 ±0.170	433
550±10	-0.060	-0.471 ±0.070	543
550 ^a	-0.370	-0.390 { +0.110 -0.080	628
599±13	+0.395	-0.370 ±0.151	433
600±12.5	+0.174	-0.469 ±0.100	509
600±11.5	+0.078	-0.538 ±0.092	543
600±11.5	-0.203	-0.780 ±0.060	628
649±17	+0.450	-0.454 ±0.182	433
650±12.5	-0.070	-0.811 ±0.045	628
712±17	+0.467	-0.33 ±0.174	455
700±16	+0.342	-0.598 ±0.106	509
700±14	+0.267	-0.647 ±0.106	543
700±14.5	+0.044	-0.834 ±0.070	628
700±12.5	-0.113	-0.870 ±0.056	684
747±21.5	+0.566	-0.245 ±0.194	433
750±14.5	+0.403	-0.312 ±0.097	509
750±15.5	+0.334	-0.301 ±0.086	543
748±16.5	+0.131	-0.653 ±0.065	628
754±15	-0.002	-0.571 ±0.040	684
800±21	+0.457	-0.197 ±0.117	509
800±20.5	+0.392	-0.068 ±0.080	543
800±18	+0.213	-0.155 ±0.062	628
850±18	+0.503	+0.092 ±0.115	509
847±19	+0.276	-0.057 ±0.053	628
850±17.5	+0.156	-0.160 ±0.058	684
910±30	+0.627	-0.180 ±0.300	455
900±20	+0.583	+0.339 ±0.100	509
897±23	+0.331	-0.031 ±0.089	628
901±25	+0.222	-0.108 ±0.062	684
950 ^b	+0.375	-0.245 ±0.095 ^b	628
950±27	+0.276	-0.191 ±0.133	684
1000±23	+0.604	+0.108 ±0.166	509
570±11	-0.267	-0.548 ±0.062	628
970±27	+0.399	-0.328 ±0.096	628

^a Extrapolated from 570-MeV point at fixed proton momentum.

^b Extrapolated from 970-MeV point at fixed proton momentum.

to zero). The corrected polarization for elastically scattered protons at 900 MeV and $10F^{-2}$ was $1.3 \pm 2.0\%$.

Table III gives the final data for the 44-in. spectrometer experiments, and Table IV gives the data for the 100-in. spectrometer experiments. The laboratory photon energy and photon energy half-width at half maximum (HWHM) appear in the first column of the tables. The half-width was computed (with a few exceptions) from the 3% (full width, FW) momentum acceptance and 1.2° (FW) angular acceptance in the 44-in. magnet experiment and from the 2% (FW) momentum and 1.0° (FW) angular acceptance in the 100-in. magnet experiment. The cosine of the pion c.m. angle appears in the second column, the measured polarization and its uncertainty in the third, and the spectrometer momentum in the last column. The uncertainty in the polarization, ΔP , is given by combining the statistical uncertainty ΔP_{stat} based on the number of scattering events, with the systematic uncertainty in the mean analyzing power,

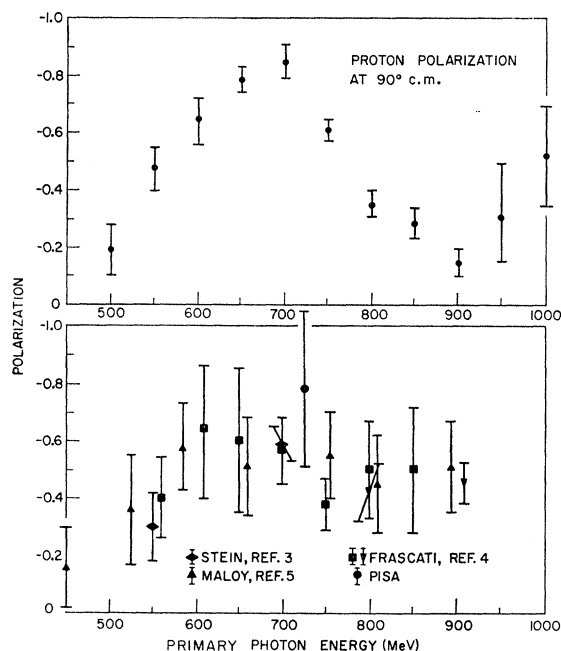


FIG. 6. (a) Our results for the proton polarization measured at 90° c. m. versus primary photon energy; (b) previous polarization measurements of all other laboratories for comparison purposes.

$\Delta\bar{f}/\bar{f}$, which appears in the last column of Table I;

$$\left(\frac{\Delta P}{P}\right)^2 = \left(\frac{\Delta P_{\text{stat}}}{P}\right)^2 + \left(\frac{\Delta\bar{f}}{\bar{f}}\right)^2. \quad (6)$$

However, the statistical uncertainty always outweighed the systematic uncertainty. Positive values of polarization are defined relative to $\mathbf{k}_{\text{photon}} \times \mathbf{q}_{\text{pion}}$.

TABLE IV. Tabulation of polarization measurements taken with the 100-in. spectrometer. Positive values of polarization are defined relative to $\mathbf{k}_{\gamma} \times \mathbf{q}_{\pi}$ in both Tables III and IV.

Primary photon energy K_{γ} and resolution (HWHM) in MeV	$\cos\theta_{\pi}^{\text{c.m.}}$	Experimental polarization values	Spectrometer momentum (MeV/c)
609 ± 6.7	-0.655	-0.747 ± 0.091	756
660 ± 7.6	-0.472	-0.824 ± 0.078	756
657 ± 7.5	-0.679	-0.970 ± 0.108	831
706 ± 14.5	+0.460	-0.47 ± 0.162	459
711 ± 8.0	-0.313	-0.974 ± 0.085	756
709 ± 9.0	-0.550	-0.936 ± 0.106	831
761 ± 11.0	-0.186	-0.590 ± 0.066	756
760 ± 10.0	-0.396	-0.802 ± 0.081	831
814 ± 14.0	-0.084	-0.407 ± 0.059	756
811 ± 11.0	-0.272	-0.407 ± 0.056	831
867 ± 17.0	+0.010	-0.271 ± 0.054	756
857 ± 13.5	-0.174	-0.430 ± 0.067	831
914 ± 20.0	+0.079	-0.149 ± 0.047	756
912 ± 15.0	-0.085	-0.120 ± 0.055	831
968 ± 23.0	+0.143	-0.272 ± 0.098	756
1018 ± 28.0	+0.201	-0.427 ± 0.084	756

7. COMPARISON WITH PREVIOUS DATA

Figure 6(a) shows the polarization at 90° c.m. measured as a function of the primary photon energy. For each energy we interpolated between the measured data points in the c.m. angular distribution to find the 90° c.m. polarization, and this is displayed as a function of photon energy in Fig. 6(a). Figure 6(b) shows all previous polarization data. These data were all taken at or near 90° c.m. While the previous data are in general agreement, they do not show the pronounced dip in the polarization values at primary photon energies of 900 MeV.

The lack of agreement of the Frascati⁴ data with this experiment, near 900 MeV, can be largely accounted for by the comparatively poor photon energy resolution of their experiment. Each Frascati datum point is an average polarization over a wide range of photoproduction kinematics, weighted according to the π^0 cross section. The narrow dip in both the cross section and polarization at 900 MeV would not be expected to be clearly resolved in their experiment. Similarly, disagreement of the data of Maloy *et al.*⁵ at 900 MeV probably stems from a similar lack of resolution resulting from the introduction of beryllium absorber in front of their spectrometer to slow down protons produced at high momenta.

Recent results of Bloom¹⁸ from the California Institute of Technology are in agreement with our results at photon energies of 800–900 MeV near 60° c.m. angle.

For the polarization $P(k, \theta_{\pi})$ written in the form of Eq. (1),

$$P(k, \theta_{\pi}) d\sigma(k, \theta_{\pi}) / d\Omega = \frac{\sin\theta_{\pi}}{\sin\theta_{\pi}} = A(k) + B(k) \cos\theta_{\pi} + C(k) \cos^2\theta_{\pi} + \dots \quad (1)$$

Figure 7 shows the coefficients $A(k)$ and $B(k)$ as determined by a least-squares fit to the data at each primary photon energy k . In the energy range of 600–800 MeV, the differential cross section $d\sigma(k, \theta_{\pi})/d\Omega$ was taken from the data of de Staebler, Erickson, Hearn, and Schaefer,¹⁹ of Diebold,⁷ and of Berkelman.²⁰ At $k=850$ and 900 MeV, we have used rough values obtained from our own data.

8. DISCUSSION OF RESULTS

There have been a number of theoretical treatments of proton polarization in photoproduction. Sakurai²¹ first pointed out the possibility of making an assign-

¹⁸ Elliott Bloom, Ph.D. thesis, California Institute of Technology, 1967 (unpublished).

¹⁹ H. de Staebler, E. F. Erickson, A. C. Hearn, and C. Schaefer, Phys. Rev. **140**, B336 (1965).

²⁰ Karl Berkelman and James A. Waggoner, Phys. Rev. **117**, 1364 (1960).

²¹ J. J. Sakurai, Phys. Rev. Letters **1**, 258 (1958).

ment of the parity of the second pion-nucleon resonance by making an experimental measurement of the recoil proton polarization at 700-MeV photon energy and at 90° c.m. Stein³ made such measurements, and in 1961 Peierls² proposed a three-resonance model to account for pion-photoproduction measurements below 1-GeV photon energy.

Since that time, a large body of more accurate photoproduction data taken with higher resolution and with better statistical accuracy has brought about the need for much more detailed analyses of pion photoproduction. Such analyses are being carried out by several authors.²²⁻²⁴ While qualitative discussion cannot be a substitute for these detailed analyses, some features of the data are worth noting. The coefficient $A(k)$ has a large peak at energies just below the energy at which the peak of the "second resonance" cross section occurs. This appears to arise from the interferences of the P_{33} and D_{13} states and has been noted before.^{3,21}

The $B(k)$ coefficient is large at 800 and 850 MeV in the neighborhood of the $S_{11}(1530)$ resonance and drops sharply at 900 MeV, suggesting an interference between the $D_{13}(1512)$ and $S_{11}(1530)$ resonances.

The long tail of the $A(k)$ coefficient below 700 MeV and the large $B(k)$ coefficient below 700 MeV could be attributed to the effects of a P_{11} resonance. The analysis of Chau *et al.*²³ does, indeed, accord with this explanation. However, other explanations cannot be ruled out.

9. CONCLUSIONS

New data are presented on the angular and energy dependence of the polarization of the recoil protons produced by π^0 photoproduction from hydrogen.

With the better angular and energy definition of this experiment, we observed structure that had not been seen previously. In particular, the 90° c.m. polarization dips to a value close to zero at primary photon energies around 900 MeV.

We have also measured angular distributions for the polarization. These angular distributions showed strong

²² R. L. Walker (private communication).

²³ Y. C. Chau, Norman Dombey, and R. G. Moorhouse (private communication).

²⁴ W. Schmidt and G. Schmidevski (private communication).

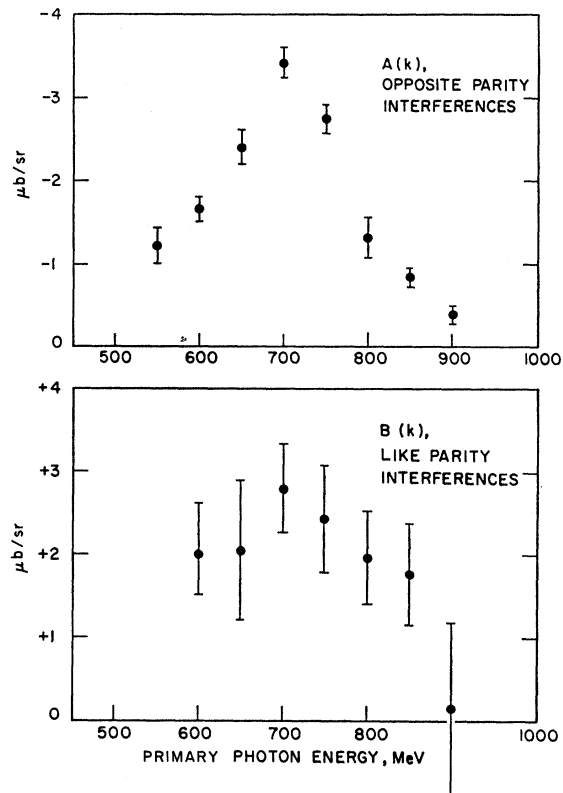


Fig. 7. Coefficients $A(k)$ and $B(k)$ appearing in Eq. (1) in units of $\mu\text{b}/\text{sr}$ plotted against the primary photon energy in MeV.

angular dependences, characteristic of interferences between states of like parity, between 600 and 850 MeV. Our data have been included in recent phase-shift analyses for photoproduction data.²²⁻²⁴

ACKNOWLEDGMENTS

We would like to thank the Mark III accelerator operators and crew under Dr. Perry Wilson and Gordon Gilbert for many hours of efficient operation at high beam intensity. Also we would like to thank John Grant, Lynn Boyer, and Peter Zihlmann for their invaluable technical assistance. One of us (D.E.L.) would like to thank the Office of Naval Research (Contract No. Nonr 225-67) for fellowship support for four years.